Mater. Res. Soc. Symp. Proc. Vol. 1407 © 2012 Materials Research Society
DOI: 10.1557/opl.2012.464

Raman Spectroscopy on Individual Identified Carbon Nanotubes

R. Parret[1,2], D. Levshov[1,2,3], T. X. Than[1,2,4], D. Nakabayashi[1,2], T. Michel[1,2], M. Paillet[1,2], R. Arenal[5,6], V. N. Popov[7], V. Jourdain[1,2], Yu. I. Yuzyuk[3], A. A. Zahab[1,2], and J.-L. Sauvajol[1,2]
[1]Université Montpellier 2, Laboratoire Charles Coulomb, F-34095 Montpellier, France
[2]CNRS, Laboratoire Charles Coulomb, F-34095 Montpellier, France
[3]Faculty of Physics, Southern Federal University, Rostov-on-Don, Russia
[4]Laboratory of Carbon Nanomaterials, Institute of Materials Science, VAST, Hanoi, Vietnam
[5]Laboratorio de Microscopias Avanzadas (LMA), Instituto de Nanociencia de Aragon (INA), Universidad de Zaragoza, 50018 Zaragoza, Spain
[6]Laboratoire d'Etude des Microstructures, ONERA-CNRS, 92322 Chatillon, France
[7]Faculty of Physics, University of Sofia, BG-1164 Sofia, Bulgaria

ABSTRACT

In this paper, we discuss the low-frequency range of the Raman spectrum of individual suspended index-identified single-walled (SWCNTs) and double-walled carbon nanotubes (DWCNTs). In SWCNTs, the role of environment on the radial breathing mode (RBM) frequency is discussed. We show that the interaction between the surrounding air and the nanotube does not induce a RBM upshift. In several DWCNTs, we evidence that the low-frequency modes cannot be connected to the RBM of each related layer. We discuss this result in terms of mechanical coupling between the layers which results in collective radial breathing-like modes. The mechanical coupling qualitatively explains the observation of Raman lines of radial breathing-like modes, whenever only one of the layers is in resonance with the incident laser energy.

INTRODUCTION

Raman measurements on macroscopic ensembles of individualized luminescent semiconducting single-walled carbon nanotubes (SWCNTs), allowed establishing a radial breathing modes (RBM) vs. diameter relationship based on (n,m) assignments from photoluminescence data [1]. In other studies performed on the same kind of samples, the (n,m) indexing of SWNTs was obtained from the best matching between experimental resonance energies and calculated transition energies obtained in the framework of different tight binding approaches. The former was derived from measurements of the RBM excitation profile of a large number of SWCNTs (both semiconducting and metallic) by resonant Raman spectroscopy (RRS). In this way, relationships between RBM frequency and nanotubes' diameter were derived [2,3,4,5]. More recently, measurements on macroscopic ensembles of SWCNTs, enriched in a specific chirality, permit to discuss the profile of the G-modes of this kind of SWCNTs [6,7]. However, the combination of high resolution transmission microscopy (HRTEM), electron diffraction (ED) and RRS on an individual, spatially isolated, suspended nanotube is the ultimate method to determine unambiguously its structural parameters, optical transitions and Raman-active phonon modes. We successfully used this combination to determine the RBM and the G bands features, as well as to evaluate the transition energies of individual, achiral and chiral,

semiconducting and metallic index-identified suspended SWCNTs [8-12]. The same approach has also been used to measure the RBM of few metallic individual SWCNTs [13]. Combined Rayleigh scattering and ED experiments have also permitted to determine the optical transitions of individual index-identified SWCNTs [14].

Double-walled carbon nanotubes (DWCNTs) are more complex systems than SWCNTs. First, the inner and outer can be either metallic (M) or semiconducting (SC) and then four different configurations are possible, namely: SC@SC, SC@M, M@SC and M@M. Second, the properties of DWCNTs are dependent on the individual nature and properties of each layer and on layer interactions. Third, it was also found that a same (n,m) inner tube can be contained inside different outer tubes [14] leading to different strengths in the layer interactions. Among the different layer interactions, coupled vibrations of the system formed by the inner and outer layer can be studied by Raman spectroscopy, especially in the low-frequency range. Measurements on DWCNTs have been mainly performed on macroscopic ensembles of DWCNTs [15-17]. Some results were also obtained on individual DWCNTs deposited on a substrate [17,18].

In this paper, we focus on the results obtained on the low-frequency range of individual, spatially isolated, SWCNTs and DWCNTs, most of these tubes being index-identified from ED. We particularly demonstrate for some DWCNTs the role of the mechanical coupling between the layers on the frequency and Raman resonance conditions of the radial breathing like modes (RBLM).

EXPERIMENTAL DETAILS

The investigated individual SWCNT and DWCNTs used in this study were synthesized by chemical vapor deposition (CVD) directly across a slit microfabricated on a Si substrate, or onto a Si_xN_y grid with holes (2 μm in diameter).

TEM, HRTEM and ED patterns were recorded in a FEI Titan microscope operating at 80 kV to reduce damages induced by electron irradiation. For the same reason, TEM images and ED patterns were recorded within an average 5 s acquisition times.

Resonant Raman scattering measurements were carried out using a Jobin Yvon T64000 spectrometer equipped with a liquid nitrogen-cooled silicon CCD detector. The scattered light was collected through a microscope using a backscattering configuration. In all the measurements, both incident and scattered light polarizations are along the nanotube axis (// // polarized Raman spectrum). Incident excitations from Ar+ and Kr+ lasers and a tunable Ti/sapphire laser were used. In order to avoid heating effects, the laser power impinging the sample was kept below 50μW.

DISCUSSION

In the first part of this paper, the diameter dependence of the RBM frequency measured in index-identified suspended SWCNTs is reviewed [8,9,12]. A comparison of measurements performed in air and in vacuum is presented and the role of environment on the measured RBM frequency is discussed.

Raman spectroscopy of index-identified single-walled carbon nanotubes

By combining RRS and ED experiments, we measured, in air and at room temperature, the RBM frequencies of several individual semiconducting and metallic index-identified SWCNTs [8,9,12] (figure 1a, solid symbols). To fit these data, we use the "universal" relation proposed by Araujo et al.: ω_{RBM} (d) = 227/d *$(1+Cd^2)^{0.5}$ [19]. In this relation, d is the tube diameter and C is a parameter associated to the interaction between the tube and its environment. Consequently, C value is expected to be close to zero for a nanotube free of any environmental effect (figure 1a, red dashed line) giving a ω_{RBM} vs. d relation in agreement with theoretical models [20]. It is surprising to find that the fit of our data measured on suspended SWCNTs leads to a C value close to 0.065 nm^{-2} (figure1a, black solid line).

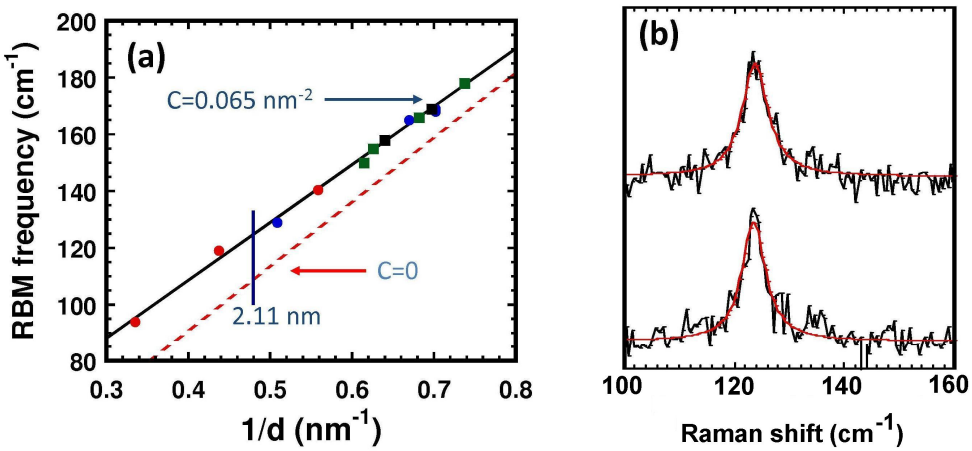

Figure 1. (a) RBM frequency vs. diameter for individual suspended SWCNTs. Black solid and red dashed lines correspond to different ω_{RBM} (d) relationships (see text). (b) Raman spectra of the same individual suspended SWCNT (d=2.11 nm) in air (top) and under vacuum (bottom).

Because our experiments are performed on individual suspended SWCNTs in air, the first hypothesis to explain the non-zero value of the C term is to consider the interaction between the nanotubes and the surrounding air. To test this assumption, we performed Raman experiments on the same suspended individual SWCNT in air and in vacuum (10^{-6} mbar) (figure 1b). From the measurement in air, a diameter close to 2.11 nm is derived for this SWCNT by using the previous relation. For such a diameter, a RBM downshift of about 17 cm^{-1} is expected when the tube is measured free of environment (corresponding to the C=0 curve, red dashed line in figure1a). In complete disagreement with this prediction, no measurable shift is experimentally observed under vacuum. Similar results have been obtained on three other individual SWCNTs. These experimental findings rule out the interaction between the tube and the surrounding air as the reason for the observed RBM upshift with respect to theoretical predictions [19,20].

Recently, by combining ED and Raman spectroscopy, Liu et al. have measured the diameter dependence of the RBM frequency of clean suspended index-identified SWCNTs in the diameter range 1.8-5 nm [21]. From HRTEM, it was claimed that the tubes used in this experiment were free of amorphous carbon. By contrast with our results, the diameter dependence of the RBM frequency is perfectly described by the linear relation: ω_{RBM}= 228/d [21]. This finding suggests that the origin of the upshift of RBM frequency could be assigned to the presence of amorphous carbon at the SWCNT surface. This conclusion underlines the strong dependence of the RBM

frequency of individual suspended SWCNTs on the environmental conditions. Dedicated experiments are however still needed to fully highlight the role of environment and potential contaminants.

Raman spectroscopy of index-identified double-walled carbon nanotubes

In this part, we focus on the results which unambiguously establish the role of the mechanical coupling between the layers on the phonon frequencies and resonance conditions in some DWCNTs. Especially we analyze in details the low-frequency range of the Raman spectrum of the (12,8)@(16,14) DWCNT.

Figure 2a displays the low frequency region of the Raman spectrum excited at 2.41 eV (Fig.2a, middle) and 1.92 eV (Fig.2a, bottom). For these two laser excitation energies, two strong components are observed at 133 cm^{-1} (full width at half maximum, FWHM close to 4.5 cm^{-1}) and 186 cm^{-1} (FWHM = 1.5 cm^{-1}). These modes are assigned to the in-phase and the counter-phase radial breathing modes of both layers, the so-called radial breathing-like modes (RBLMs) [22]. On the same figure is displayed the RBM range of the Raman spectrum measured on the suspended individual (12,8) SWCNT (figure 2a, top). A significant frequency shift, 11 cm^{-1}, is evidenced between the position of the high-frequency RBLM (usually assigned to the RBM of the inner tube) with respect to the RBM of the (12,8) SWCNT, located at 174.6 cm^{-1}. This shift is a clear signature of the interlayer interaction in this DWCNT.

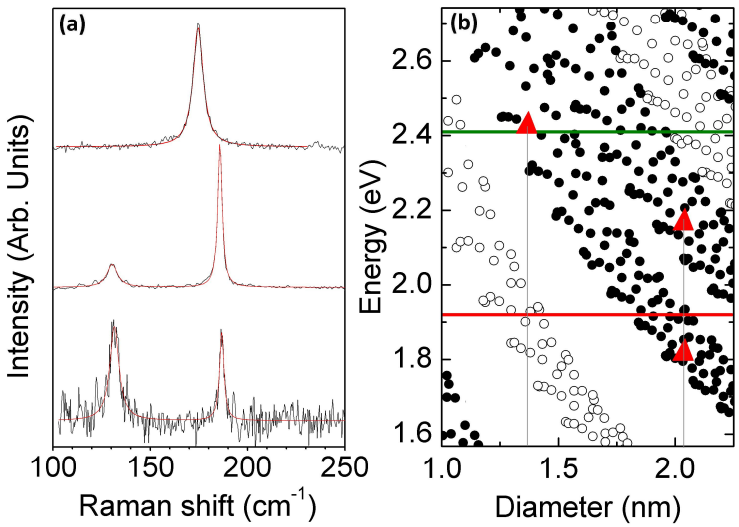

Figure 2. (a) The low frequency region of the Raman spectra of the (12,8)@(16,14] DWCNT excited at 1.92 eV (bottom) and 2.41 eV (middle), and of the (12,8) SWCNT excited at 2.41 eV (top). (b) normalized Kataura plot established for SWCNTs [10]. The transition energies for the third and fourth semiconducting transitions of the corresponding (12,8) and (16,14) SWCNTs are denoted by red triangles.

The use of the different ω_{RBM} vs. d relationships established for SWCNTs to derive the diameters of the inner and outer tubes from the RBLM frequencies leads to an underestimation of both diameters: 1.22 nm for the inner tube with the Liu's relation [21] and 1.28 nm with the Meyer's relation [8] against 1.36 nm for the (12,8) tube; for the outer tube, 1.71 nm with the

relation of Ref. [21] and 1.92 nm with the relation of Ref. [8] against 2.03 nm for the (16,14) tube. From this analysis, we can conclude that the ω_{RBM} vs. diameter relations established for suspended SWCNTs are not valid for this suspended DWCNT.

The measured/experimental RBLM frequencies can be compared with the theoretical predictions of Popov et al. [21,22] concerning the diameter dependence of the RBLMs. In this model, the shift of the RBLMs with respect to the RBM frequency of the individual inner and outer layers given by $\omega_{RBM}= 228/d$ for the inner tube and $\omega_{RBM}= 204/d+27$ for the outer tube (the presence of amorphous carbon around the outer tube, evidenced from HRTEM image [23], justifies to consider this relation), is calculated by taking into account the van der Waals interactions between the layers. Within this assumption, for an outer tube diameter of 2.02 nm, the frequency of the counter-phase mode frequency is calculated at 186 cm^{-1} and the in-phase mode around 136 cm^{-1} in close agreement with the experimental values.

The observation of the two RBLMs at the same excitation energy is striking. To understand these results, we use, as commonly done in the literature for individual MWCNTs [17,18,24], the normalized Kataura established for SWCNTs (figure 2b) [10]. Such a Kataura plot is validated by the fact that measurements of the transition energies on DWCNTs only display a slight shift with respect to the transition energies of the corresponding SWCNTs [17,25]. On this Kataura plot, the transition energies for the third and fourth semiconducting transitions of the corresponding (12,8) and (16,14) SWCNTs are denoted by red triangles on figure 2b. At 2.41 eV, the laser energy is very close to the E_{33} transition (2.43 eV) expected for the (12,8) inner tube. By contrast, no transition is expected at this energy for the (16,14) outer tube. At 1.92 eV, the difference with the E_{33}=1.85 eV of the (16,14) is small enough to assume that the outer tube is in incoming resonance at this energy. The examination of the resonance conditions for the DWCNT, on the basis of the Kataura plot, leads to conclusions which disagree with experiment. Indeed, at 2.41 eV and 1.92 eV excitation energies, only one tube of the DWCNT should be resonant though we measure two distinct RBLMs. The disagreement is resolved by considering a mechanical coupling between the two layers. In that case, only the optical resonance of one tube is necessary to observe the response of the coupled system. This mechanical coupling has already been observed on an individual bundle of two SWNTs [13]. It is directly evidenced here in the case of a DWCNT. Qualitatively, if one layer is in resonance, the coupling can induce the observation of all RBLMs of the DWCNT and a relatively small intensity of the mode affiliated to the non resonant layer is expected. Taking into account the coupling between the layers is the only way to explain coherently the present results. In consequence, the use of the Kataura plot to identify the structure of each layer in a DWCNT by means of the resonance energy and the RBLM frequencies is not straightforward. This point is illustrated hereafter by two examples.

The low frequency range of Raman spectra excited at 2.33 eV and 1.49 eV measured on a DWCNT, non identified by ED, is displayed on figure 3a. The in-phase and counter phase RBLM are located at 140 cm^{-1} and 202.5 cm^{-1}, respectively. From [23], the diameters of the layers are 1.90 nm for the outer tube and 1.22 nm for the inner tube. The presence of the two RBLMs at each excitation energy leads to assign transition energies close to 2.33 eV and 1.49 eV for both inner and outer tube. The Kataura plot of figure 3b leads to contradictory conclusions: (i) the outer layer should be semiconducting at 2.33 eV and metallic at 1.49 eV. (ii) no possible indices can be found for the inner tube at 2.33 eV.

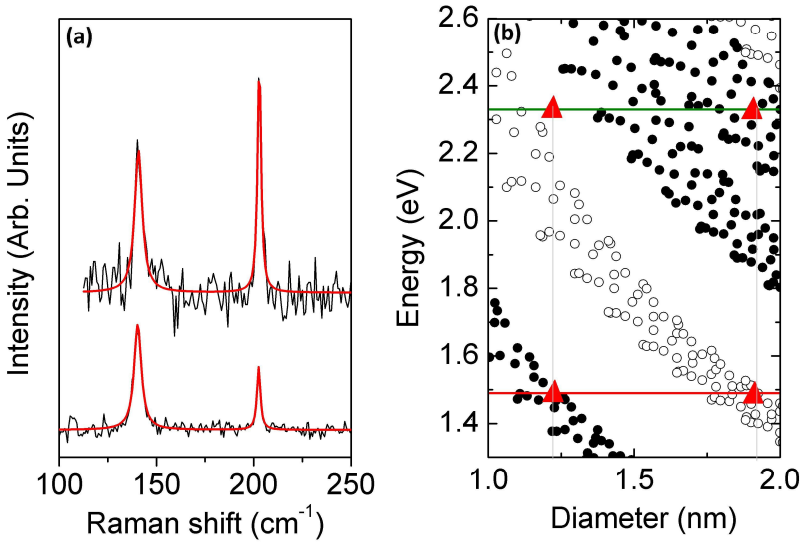

Figure 3. (a) The low frequency region of the Raman spectra of a DWCNT excited at 1.49 eV (top) and 2.33 eV (bottom). (b) Normalized Kataura established for SWCNTs [10]. The experimental resonance energies for the inner and outer tubes are denoted by red triangles.

The low frequency range of Raman spectrum excited at 1.96 eV measured on another DWCNT, non identified by ED, is displayed figure 4a. Two RBLMs are measured at 123 cm^{-1} and 170 cm^{-1} respectively, leading to following diameters: 2.20 nm for the outer tube and 1.52 nm for the inner tube.

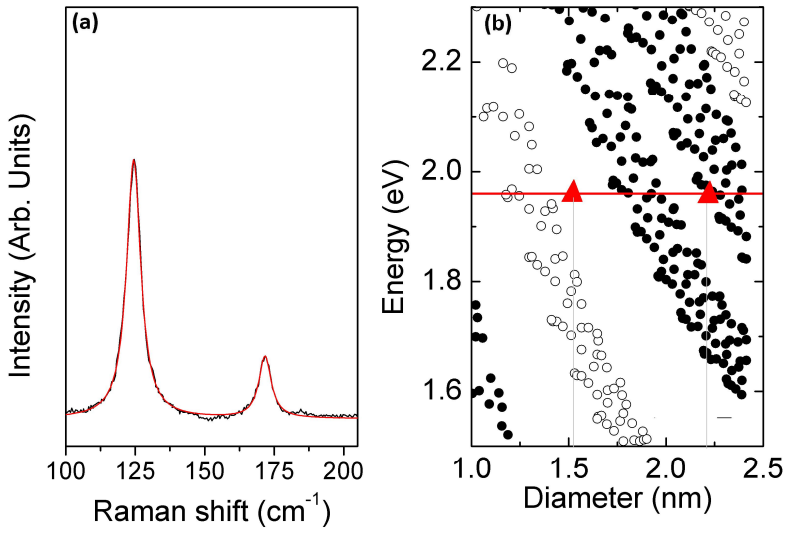

Figure 4. (a) The low frequency region of the Raman spectra of a DWCNT excited at 1.96 eV. (b) Normalized Kataura established for SWCNTs [10]. The experimental resonance energies for the inner and outer tubes are denoted by red triangles.

The observation of two RBLMs suggests transition energies close to 1.96 eV for both inner and outer tubes. Opposite to this assumption, the Kataura plot of Fig.4b does not predict any transition energy close to 1.96 eV for the inner tube. The results obtained on these two non-

index-identified DWCNTs can only be understood by considering a mechanical coupling between the two layers as the origin of the observation of two RBLMs whenever only one of the two layers is in resonance.

Theses results state that mechanical coupling can play a major role on the conditions needed for the observation of the low frequency modes in a Raman spectrum excited at a given laser energy and on the frequencies of the in-phase and counter-phase RBLMs. From a general point of view, the analysis of the Raman spectrum of DWCNT should be done by considering a possible mechanical coupling between the layers. The strength of this mechanical coupling will depend on the interlayer distance and nanotube diameter. For interlayer distances larger than 0.4 nm, a weak interaction between both layers is expected independently of the tube diameter [22]. Assuming an interlayer distance close to 0.34 nm, two coupling regimes are theoretically predicted depending on the tube diameter: For outer tube diameters smaller than ~2 nm, the vibrations of the inner and the outer tubes are independent and for outer tube diameters larger than ~2 nm, the RBLMs corresponds to collective breathing vibrations of both layers [22,23]. All the DWCNTs, discussed in this paper, belong to this later case.

CONCLUSIONS

We presented in this paper a detailed Raman study of individual suspended SWCNT and DWCNTs. Comparison between measurements in air and in vacuum on the same suspended nanotubes rule out the air-nanotube interaction as the origin for the upshift of the RBM. On the other hand, we showed that the low-frequency features, the so-called RBLM, obtained at different excitation energies on some DWCNTs can only be understood in a coherent way by considering the coupling between the two concentric layers. We can conclude that the experimental RBM frequency vs. diameter relation in SWCNTs is still not yet fully understood and that for DWCNTs a coupled vibration of the two layers can occur. This mechanical coupling could complicate the index assignment of DWCNTs from Raman spectroscopy as compared to SWCNTs.

ACKNOWLEDGMENTS

This work has been done in the framework of the GDRI (CNRS) "Graphene and Nanotubes: Science and Application". The authors acknowledge financial support from ANR Excitubes, TRAIN^2 network and French Russian PICS N°4818.

REFERENCES

1. S. M. Bachilo, M. Strano, C. Kittrell, R. H. Hauge, R. E. Smalley and R. B. Weisman, *Science* **298**, 2361 (2002).
2. C. Fantini, A. Jorio, M. Souza, M. S. Strano, M. S. Dresselhaus and M. Pimenta, *Phys. Rev. Lett.* **93**, 147406 (2004).
3. H. Telg, J. Maultzsch, S. Reich, F. Hennrich and C. Thomsen, *Phys. Rev. Lett.* **93**, 177401 (2004).
4. M. S. Strano, S. K. Doorn, E. H. Hároz, C. Kittrell, R. H. Hauge, and R. E. Smalley, *Nano Lett.* **3**, 1091 (2003).

5. P. T. Araujo, S. K. Doorn, S. Kilina, S. Tretiak, E. Einarson, S. Maruyama, H. Chacam, M. A. Pimenta and A. Jorio, *Phys. Rev. Lett.* **98**, 067401 (2007).
6. E. H. Hároz, J. G. Duque, W.D. Rice, C. G. Densmore, J. Kono and S.K. Doorn, *Phys. Rev.* B **84**, 121403(R) (2011).
7. H. Telg, J. G. Duque, M. Staiger, X. Tu, F. Hennrich, M. M. Kappes, M. Zheng, J. Maultzsch, C. Thomsen and S. K. Doorn, *ACS Nano* **6**, 904 (2012).
8. J. C. Meyer, M. Paillet, T. Michel, A. Moréac, A. Neumann, G. S. Duesberg, S. Roth and J.-L. Sauvajol, *Phys. Rev. Lett.* **95**, 217401 (2005).
9. M. Paillet, T. Michel, J.C. Meyer, V.N. Popov, L. Henrard, S. Roth and J.-L. Sauvajol, *Phys. Rev. Lett.* **96**, 257401 (2006).
10. T. Michel, M. Paillet, J.C. Meyer, V.N. Popov, L. Henrard and Sauvajol J-L, *Phys. Rev. B* **75**, 155432 (2007).
11. T. Michel, M. Paillet, J. C. Meyer, V.N. Popov, L. Henrard, P. Poncharal, A. A. Zahab and J.-L. Sauvajol, *Physica Status Solidi b* **244**, 3986 (2007).
12. T. Michel, M. Paillet, D. Nakabayashi, M. Picher, V. Jourdain, J. C. Meyer, A. A. Zahab and J.-L. Sauvajol, *Phys. Rev. B* **80**, 245416 (2009).
13. A. Débarre, M. Kobylko, A.-M. Bonnot, A. Richard, V. N. Popov, L. Henrard and M. Kociak, *Phys. Rev. Lett.* **101**, 197403 (2008).
14. M. Y. Sfeir, T. Beetz, F. Wang, L. Huang, X. M. H. Huang, M. Huang, J. Hone, S. O'Brien, J. A. Misewich, T. F. Heinz, L. Wu, Y. Zhu and L. E. Brus, *Science* **312**, 554 (2006).
15. R. Pfeiffer, F. Simon, H. Kuzmany, and V.N. Popov, *Phys. Rev. B* **72**, 161404 (2005).
16. S. Bandow, G. Chen, U. Sumanesekera, R. Gupta, M. Yudasaka, S. Iijima and P.C. Eklund, *Phys. Rev. B* **66**, 075416 (2002).
17. F. Villalpando-Paez, L. G. Moura, C. Fantini, H. Muramatsu, T. Hayashi, Y.A. Kim, M. Endo, M. Terrones, M. A. Pimenta and M. S. Dresselhaus, *Phys. Rev. B* **82**, 155416 (2010).
18. F. Villalpando-Paez, H. Son, D. Nezich, Y. P. Hsieh, J. Kong, Y. A. Kim, D. Shimamoto, H. Muramatsu, T. Hayashi, M. Endo, M. Terrones and M. S. Dresselhaus, *Nano Lett.* **8**, 3879 (2008).
19. P. T. Araujo, I. O. Maciel, P. B. C. Pesce, M. A. Pimenta, S. K. Doorn, H. Quian, A. Hartschuh, M. Steiner, L. Grigorian, K. Hata, and A. Jorio, *Phys. Rev. B* **77**, 241403 (2008).
20. G. D. Mahan, *Phys. Rev. B* **65**, 235402 (2002).
21. K. Liu, W. Wang, M. Wu, F. Xiao, X. Hong, S. Aloni, X. Bai, E. Wang and F. Wang, *Phys. Rev. B* **83**, 113404 (2011).
22. V. N. Popov and L. Henrard, *Phys. Rev. B* **65**, 235415 (2002).
23. D. Levshov, T. X. Than, R. Arenal, V. N. Popov, R. Parret, M. Paillet, V. Jourdain, A. A. Zahab, T. Michel, Yu. I. Yuzyuk, and J.-L. Sauvajol, *Nano Lett.* **11**, 4800 (2011).
24. C. Spudat, M. Müller, L. Houben, J. Maultzsch, K. Goss, C. Thomsen, C. M. Schneider, and C. Meyer, *Nano Lett.* **10**, 4470 (2010).
25. T. Hertel, A. Hagen, V. Talalaev, K. Arnold, F. Hennrich, M. Kappes, S. Rosenthal, J. McBride, H. Ulbricht and E. Flahaut, *Nano Lett.* **5**, 511 (2005).